CLINICS

ORIGINAL ARTICLE

Effects and mechanism of stem cells from human exfoliated deciduous teeth combined with hyperbaric oxygen therapy in type 2 diabetic rats

Yifeng Xu [I,II,#], Jin Chen,[I,#] Hui Zhou,[III] Jing Wang,[I,IV] Jingyun Song,[I] Junhao Xie,[I] Qingjun Guo,[I] Chaoqun Wang,[I] Qin Huang [I,*]

[I] Department of Endocrinology, Changhai Hospital, the First Affiliated Hospital of the Naval Medical University, Shanghai 200433, China. [II] Department of Endocrinology, Air Force Hospital of Northern Theater Command of PLA, Shenyang 110042, China. [III] Department of Out-patient, Changning retired cadre retreat of Shanghai garrison command, Shanghai 200050, China. [IV] Department of Internal Medcine, Hotan Country People's Hospital of Xinjiang, Hotan Country 848000, China.

Xu Y, Chen J, Zhou H, Wang J, Song J, Xie J, et al. Effects and mechanism of stem cells from human exfoliated deciduous teeth combined with hyperbaric oxygen therapy in type 2 diabetic rats. Clinics. 2020;75:e1656

*Corresponding author. E-mail: qxinyi1220@163.com

[#]Co-first authors

OBJECTIVES: Mesenchymal stem cells (MSCs) are potentially ideal for type 2 diabetes treatment, owing to their multidirectional differentiation ability and immunomodulatory properties. Here we investigated whether the stem cells from human exfoliated deciduous teeth (SHED) in combination with hyperbaric oxygen (HBO) could treat type 2 diabetic rats, and explored the underlying mechanism.

METHODS: SD rats were used to generate a type 2 diabetes model, which received stem cell therapy, HBO therapy, or both together. Before and after treatment, body weight, blood glucose, and serum insulin, blood lipid, pro-inflammatory cytokines (tumor necrosis factor-alpha and interleukin-6), and urinary proteins were measured and compared. After 6 weeks, rats were sacrificed and their organs were subjected to hematoxylin and eosin staining and immunofluorescence staining for insulin and glucagon; apoptosis and proliferation were analyzed in islet cells. Structural changes in islets were observed under an electron microscope. Expression levels of *Pdx1*, *Ngn3*, and *Pax4* mRNAs in the pancreas were assessed by real-time quantitative polymerase chain reaction (RT-qPCR).

RESULTS: In comparison with diabetic mice, those treated with the combination or SHE therapy showed decreased blood glucose, insulin resistance, serum lipids, and pro-inflammatory cytokines and increased body weight and serum insulin. The morphology and structure of pancreatic islets improved, as evident from an increase in insulin-positive cells and a decrease in glucagon-positive cells. Terminal deoxynucleotidyl transferase-mediated dUTP nick end labeling (TUNEL) staining of islet cells revealed the decreased apoptosis index, while Ki67 and proliferating cell nuclear antigen staining showed increased proliferation index. Pancreatic expression of *Pdx1*, *Ngn3*, and *Pax4* was upregulated.

CONCLUSION: SHED combined with HBO therapy was effective for treating type 2 diabetic rats. The underlying mechanism may involve SHED-mediated increase in the proliferation and trans-differentiation of islet β-cells and decrease in pro-inflammatory cytokines and apoptosis of islets.

KEYWORDS: Type 2 Diabetic Rats; SHED; Stem Cell Therapy; Hyperbaric Oxygen Therapy; Immunoregulation.

INTRODUCTION

Diabetes is the 11th most common cause of disability worldwide, and serves as a high risk factor for cardiovascular disease. According to the International Diabetes Federation (IDF) (1), more than 425 million people worldwide had diabetes in 2017 and this number is expected to increase to 625 million by 2045. In 2017 alone, diabetes and its complications killed more than 4 million people and were associated with a treatment cost of $727 billion. Diabetes has emerged as a serious global and social public health problem and is a heavy social and economic burden. Type 2 diabetes (T2DM) accounts for about 90 percent of all diabetes cases. It is mainly caused by insulin resistance and islet cell dysfunction. The current medicines and treatment regimens are ineffective in preventing the spread and development of diabetes and its complications. Stem cell and regenerative medicine technology has exploited the multi-directional differentiation, autocrine and paracrine, immune regulation, and other characteristics of mesenchymal stem cells (MSCs)

Copyright © 2020 **CLINICS** – This is an Open Access article distributed under the terms of the Creative Commons License (http://creativecommons.org/licenses/by/4.0/) which permits unrestricted use, distribution, and reproduction in any medium or format, provided the original work is properly cited.

No potential conflict of interest was reported.

Received for publication on November 28, 2019. **Accepted for publication on** February 10, 2020

DOI: 10.6061/clinics/2020/e1656

to repair or replace the function of a damaged pancreatic tissue, thereby raising our hopes for diabetes treatment.

Dental pulp MSCs have been studied in animal models of different diseases (2), including systemic lupus erythematosus, ischemic brain injury, spinal cord injury, and muscular atrophy. Stem cells from human exfoliated deciduous teeth (SHED) were shown to differentiate into insulin-secreting cells *in vitro* (3), and may be potentially useful for the treatment of glucose metabolic disorders. Hyperbaric oxygen (HBO) therapy could increase the concentration of nitric oxide synthase, and promote mobilization of stem cells and release of endothelial progenitor cells (4). These cells may migrate to inflammatory or injured sites in the presence of inflammatory factors or chemokines (5). Oxygen regulation may also promote the maturation of pancreatic progenitor cells (6), and HBO may promote the survival and growth of transplanted islet cells by improving local oxygen supply (7). Therefore, the combination of stem cells and HBO therapy may play a plausible synergistic role in the therapy for diabetes (8,9).

MATERIALS AND METHODS

Animal model and groups

All animal experiments were approved by the Ethics Committee for Medical Laboratory Animal Sciences of Changhai Hospital of Shanghai (approval No. 201700632). Male Sprague Dawley (SD) rats weighing 90–100 g were obtained from the experimental animal center of Naval Medical University. All rats were housed at 25°C ± 1°C on a 12h light/dark cycle and fed *ad libitum* for 1 week before study inception. Animals were then fed with a high-fat diet (40% fat, 40% carbohydrate, and 20% protein) for 8 weeks, and a diabetic rat model was generated through a single intraperitoneal injection of streptozotocin (STZ, Sigma, USA) at 30 mg/kg body weight in sodium citrate buffer (pH 4.2) after overnight fasting. Blood glucose (BG) concentration was measured using a drop of tail capillary blood by a glucometer. Fasting blood glucose (FBG) $\geqslant$8.3mmol/L after 3 days, or BG 2h post oral glucose tolerance test (OGTT) after 3 days or a stable non-fasting BG concentration $\geqslant$11.1 mmol/L for 7 days, were indicative of the successful establishment of the T2DM rat model (10).

T2DM rats were randomly divided into four groups as follows: Stem cell therapy group (SC, n=6), HBO therapy group (HBO, n=6), stem cells combined with HBO group (SC + HBO, n=6), and diabetes control group (DM, n=6). Normal rats on normal diet were set as the normal control group (NC, n=6).

Stem cell therapy

SHED from P4 to P6 were supplied free of charge by CAR-T (Shanghai) Biotechnology Co., Ltd, at a density of 1×10^7 cells/mL. The expression of surface marker CD90 on MSCs was analyzed (>95%) by flow cytometry; CD34 and HLA-DR expression was low but could be detected in about 0.5% cells. Rats from SC and SC + HBO groups were transfused with 0.5 mL SHED through their caudal veins in the first and third week (twice), while rats from the other groups were transfused with an equal volume of sodium chloride.

HBO therapy

HBO therapy was performed in the diving medical laboratory of the department of marine medicine of Naval Medical University. Rats from HBO and SC + HBO groups received HBO therapy daily for a total of 28 sessions. Animals were exposed to an atmospheric pressure of 2 at an oxygen concentration of $\geqslant$85% for 1h daily in an HBO chamber (DWC-1000-2100, No. 701 Yangyuan Medical Oxygen Chamber Factory, Shanghai). The HBO chamber was first filled with pure oxygen for 3 min and then gradually pressurized for 10 min from 0 to 0.1 MPa. The pressure in the chamber was maintained at 0.1 MPa for 1h, after which the chamber was gradually decompressed for 15 min from 0.1 to 0 MPa.

Biochemical assays and enzyme-linked immunosorbent assay (ELISA)

Rats were sacrificed after 6 weeks of therapy. During treatment period, body weight of rats was measured every week and OGTT was performed every 2 weeks following overnight fasting. Glucose was intragastrically administered (2 g/kg body weight), and BG and serum insulin levels were detected at 0, 30, 60, 90, and 120 min. BG level was measured by a glucometer (Rightest GM300, Huaguang Biotech Co. LTD, Taiwan) using glucose oxidase assay. Serum insulin levels were measured using an ELISA (CUSABIO, Wuhan), while serum lipid (total cholesterol [TC], triglyceride [TG], low-density lipoprotein cholesterol [LDL-C], and high-density lipoprotein cholesterol [HDL-C]) and 24h urinary protein levels were measured using a fully automatic biochemical analyzer (Chemray 240, Rayto Life and Analytical Sciences Co., Ltd, Shenzhen) according to the manufacturer's protocols. Serum interleukin (IL)-6 and tumor necrosis factor (TNF)-α levels were measured using rat ELISA kits (Lianke Bio, Hangzhou). Area under the curves (11) for BG or insulin were calculated as follows: $AUC_{BG\ 0\text{-}120}$ (mmol/L · h) = ([BG0′ + BG30′] × 30/60)/2 + ([BG30′ + BG60′] × 30/60)/2 + ([BG60′ + BG90′] × 30/60)/2 + ([BG90′ + BG120′] × 30/60)/2; $AUC_{INS0\text{-}120}$ (nIU/mL · h) = ([INS0′ + INS30′] × 30/60)/2 + ([INS30′ + INS60′] × 30/60)/2 + ([INS60′ + INS90′] × 30/60)/2 + ([INS90′ + INS120′] × 30/60)/2. Homeostasis model assessment of insulin resistance (HOMA-IR) was calculated as follows: HOMA-IR = INS0′ (μU/mL) × BG0′ (mmol/L)/22.5.

Histopathological analysis

Sections of pancreas samples were stained with hematoxylin and eosin (H&E) and examined under a light microscope. Ultrastructure of intracellular organelles in β-cells was detected by transmission electron microscopy (HT7700, HITACHI), and particles were counted by Image-pro Plus 6.0 (IPP, Media Cybernetics, Inc.) software.

Insulin and glucagon in pancreatic islets were analyzed by immunohistochemical staining using insulin mouse mAb and glucagon rabbit mAb, respectively (Wuhan Servicebio technology), as well as by immunofluorescence staining using sheep anti-rabbit IgG-fluorescein isothiocyanate (FITC; Abcam), sheep anti-mouse IgG-CY3 (Sigma), and 4′,6-diamidino-2-phenylindole (DAPI; Sigma). Staining was observed by fluorescence microscopy (DP80, Olympus bx-53). Image-pro Plus 6.0 (IPP, Media Cybernetics, Inc.) software was used to count positively stained cells, and integrated optical density (IOD) of positive staining for insulin or glucagon was calculated and analyzed in immunofluorescence sections of the pancreas. Mean optical density (MOD) was calculated (MOD = IOD SUM/area) and compared. After 6 weeks of therapy, three islets from each pancreas tissue were analyzed for MOD of insulin and glucagon.

The serial pancreatic sections were evaluated for apoptotic cells in islets by terminal deoxynucleotidyl transferase-mediated dUTP nick end labeling (TUNEL) assay (In Situ Cell Death Detection Kit, Roche), while proliferative cells were detected with proliferating cell nuclear antigen (PCNA) and Ki67 (rabbit mAbs for anti-PCNA and anti-Ki67; Abcam). Apoptosis index (AI) and proliferation index (PI) were calculated as follows: AI = Number of apoptotic cells/(Number of apoptotic cells + Number of normal cells); PI = Number of proliferative cells/(Number of proliferative cells + Number of normal cells). After 6 weeks of therapy, three islets from rat pancreas were analyzed for AI and PI.

Real-time quantitative polymerase chain reaction (RT-qPCR)

The mRNA expression levels of *Pdx1*, *Ngn3*, and *Pax4* in the pancreas were quantified by RT-qPCR using the SYBR Green method. Rats were sacrificed and their pancreas were excised and lysed using Trizol reagent (Invitrogen) to extract RNA. Total RNA was identified and measured using a spectrophotometer (Nanodrop 1000, USA). The genes were amplified using a 96-well gradient PCR amplification apparatus (ABI Veriti, USA). Target genes were quantified by a real-time detector (Roche LightCycler® 480II, Switzerland). Glyceraldehyde 3-phosphate dehydrogenase (*GAPDH*) was used as the reference gene. PCR primers were synthesized by Sangon Biotech Co. Ltd. Shanghai. PrimeScript reverse-transcription kit and Premix ExTaq were obtained from Takara, Japan.

Primer sequences were designed using the Oligo Primer Analysis Software (Version: 7.60, Wojciech & Piotr Rychlik, USA), and their specificity was verified on the website of Primer-blast.

Oligo Name: *Pdx1* Sequence (5′ to 3′)
Forward primer GCACAAGAGCCAGTTGGGTA Plus
Reverse primer ATTGTCCTCAGTTGGGAGCC Minus
Product length 175
Oligo Name: *Pax4*
Forward primer ACAGATGCCAGGTGCTTCTC Plus
Reverse primer ATGATGCACAGGATGGGTGG Minus
Product length 292
Oligo Name: *Ngn3*
Forward primer ATGACAGAAGGGGCCAAAGG Plus
Reverse primer GTAACGGAGTGGAACCAGCA Minus
Product length 84
Oligo Name: *GAPDH*
Forward primer AGTGCCAGCCTCGTCTCATA
Reverse primer GATGGTGATGGGTTTCCCGT
Product length 248

Statistical analysis

All measurement data are expressed as the mean ± standard deviation. Before analysis, the data were tested for normality of distribution using the Kolmogorov-Smirnov test. For normally distributed data, differences between groups were analyzed using the least-significant difference test. A value of $p<0.05$ was considered statistically significant. SPSS 22.0 (IBM) was used for statistical analyses.

RESULTS

General conditions and measurement indicators

All rats were included for analysis (n=6 in each group). After treatment, the mental state of the rats from SC + HBO and SC groups was better than that of rats from DM group. Water consumption and urination significantly reduced and body weights increased for the rats from SC + HBO and SC groups (Figure 1A). Further, BG level gradually decreased (Figure 1B), serum insulin secretion increased (Figure 1C), and HOMA-IR (Figure 1D), serum LDL-C and TG (Figure 2 A), 24h urinary protein (Figure 2B), and serum TNF-α and IL-6 (Figure 2C, 2D) reduced in these groups as compared with those in DM group. The therapeutic effect in SC + HBO group appeared earlier than that in SC group.

Histopathology

Pancreatic islet morphology. After 6 weeks of therapy, the morphology of pancreatic islets was relatively intact and the number of inflammatory cells decreased in H&E-stained sections from SC + HBO and SC groups (Figure 3A). Electron microscopy revealed the improvement in the nuclear membrane integrity of organelles and the significant increase in secretory particles for SC + HBO and SC groups as compared with those for DM group (Figure 3B).

Immunofluorescence staining for insulin or glucagon in pancreatic islets. After the 6-week therapy, the MOD for insulin immunofluorescence staining in pancreatic islets was significantly higher for SC + HBO and SC groups than that for DM group, while the MOD values for glucagon in SC + HBO and SC groups were lower than the value for DM group (Figure 4A, 4B).

Apoptosis and proliferation of pancreatic islet cells. After 6 weeks of therapy, apoptosis significantly reduced and proliferation significantly increased for the islet cells from SC + HBO and SC groups as compared with those for the islets cells from DM group (Figure 5A, 5B).

RT-qPCR. The quantitative expression of pancreatic *Pdx1*, *Pax4*, and *Ngn3* mRNAs was analyzed after 6 weeks of therapy. All six rats from each group were used for RT-qPCR. Gene expression was significantly upregulated in the samples from SC + HBO and SC groups as compared with that in samples from DM group. The expression of these genes in SC + HBO group was higher than that reported in SC group (Figure 6).

DISCUSSION

In 2003, Professor Shi Songtao discovered dental pulp stem cells in his 6-year-old daughter's deciduous teeth and named them as SHED. These cells originate from the cranial neural crest and express surface molecules or antigens for MSCs such as CD29, CD44, CD73, CD90, CD105, CD166, STRO-1, CD146, and stage-specific embryonic antigen 4 (SSEA4) (12). Differentiation may be induced in some cell types, including adipocytes, neurons, chondrocytes, and MSCs, using specific stimulation conditions (13-15). Unlike the umbilical cord or cord blood stem cells that need to be extracted at birth, dental pulp stem cells may be harvested from either deciduous or permanent teeth and easily collected without any risk of complications (16). Humans bear 20 deciduous teeth that eventually fall off. Hence, there is no ethical issue involved in their collection. SHED exhibit high proliferation and differentiation

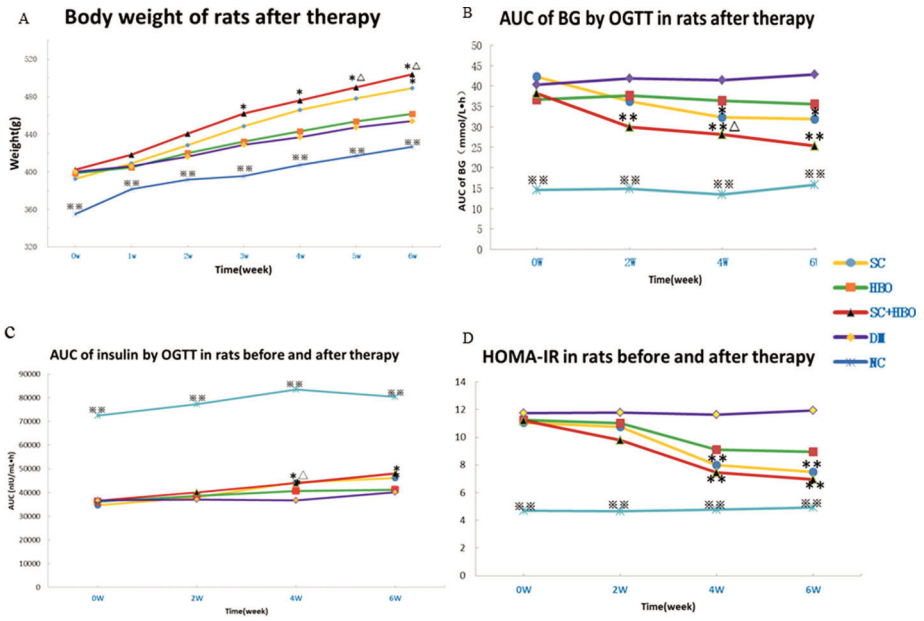

Figure 1 - Body weight and glucose metabolism indices of rats. **A**. Body weight: After 3 weeks of therapy, the body weights of the rats from the SC + HBO group were higher than those of the rats from the DM group. After 5 weeks, the body weights of the rats from the SC + HBO group were higher than those of the rats from the HBO group. After 6 weeks, the SC group rats had higher body weight than the DM group rats. B. AUC of BG by OGTT: After 2 weeks of therapy, the AUC for the rats from the SC + HBO group was lower than that for the rats from the DM group. The AUC value decreased for SC group rats as compared with that for DM group rats after 4 weeks. The AUC of SC + HBO group rats was lower than that of HBO group rats. C. AUC of INS by OGTT: After 4 weeks, the AUC started to increase for the rats from SC + HBO and SC groups as compared with that for the rats from DM group. D. HOMA-IR: After 4 weeks, the HOMA-IR for SC + HBO and SC group rats was lower than that for DM group rats. $^{*}p<0.05$, $^{**}p<0.01$ *vs* DM group, $^{\triangle}p<0.05$ *vs* HBO group. $^{**}p<0.01$ *vs* each of the other four groups.

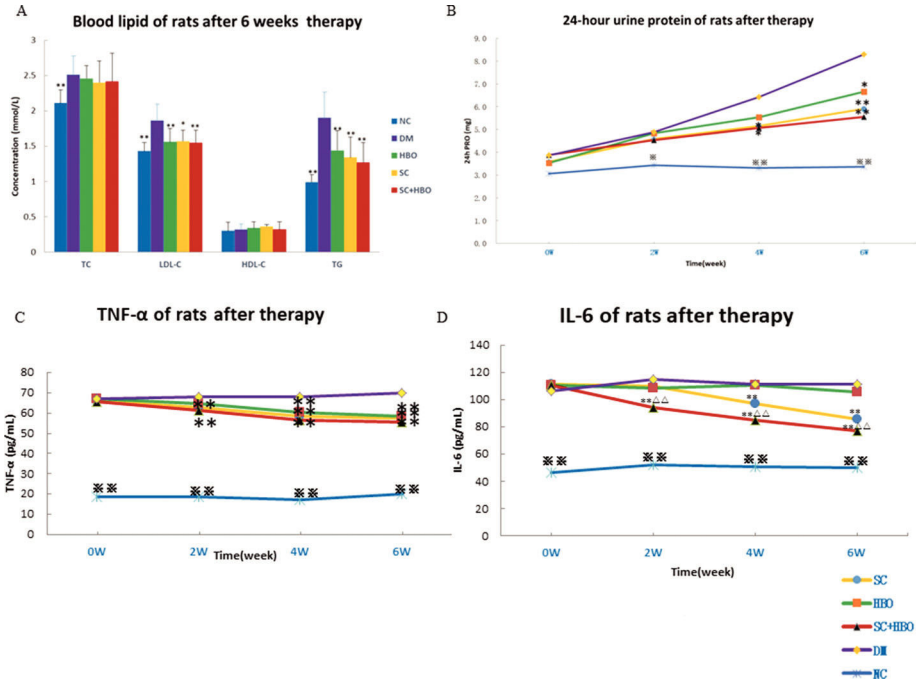

Figure 2 - Blood lipid, proinflammatory cytokine, and urine protein of rats. A. Blood lipid after 6 weeks of therapy: Serum TG and LDL levels were higher in SC + HBO, SC, and HBO groups than those in the DM group. B. 24h urine protein: After 4 weeks, urine protein levels began to decrease in SC + HBO and SC groups as compared with those in DM group. C. Serum TNF-α: After 2 weeks, serum TNF-α levels began to decrease in SC + HBO and SC groups as compared with those in the DM group. After 4 weeks, serum TNF-α level of the HBO group was lower than that of the DM group. D. Serum IL-6: After 2 weeks, serum IL-6 levels in the SC + HBO group were lower than those in DM and HBO groups. After 4 weeks, serum IL-6 levels in the SC group were lower than those in the DM group. $^{*}p<0.05$, $^{**}p<0.01$ *vs* DM group; $^{\triangle\triangle}p<0.05$ *vs* HBO group. $^{*}p<0.05$, $^{**}p<0.01$ *vs* each of the other four groups.

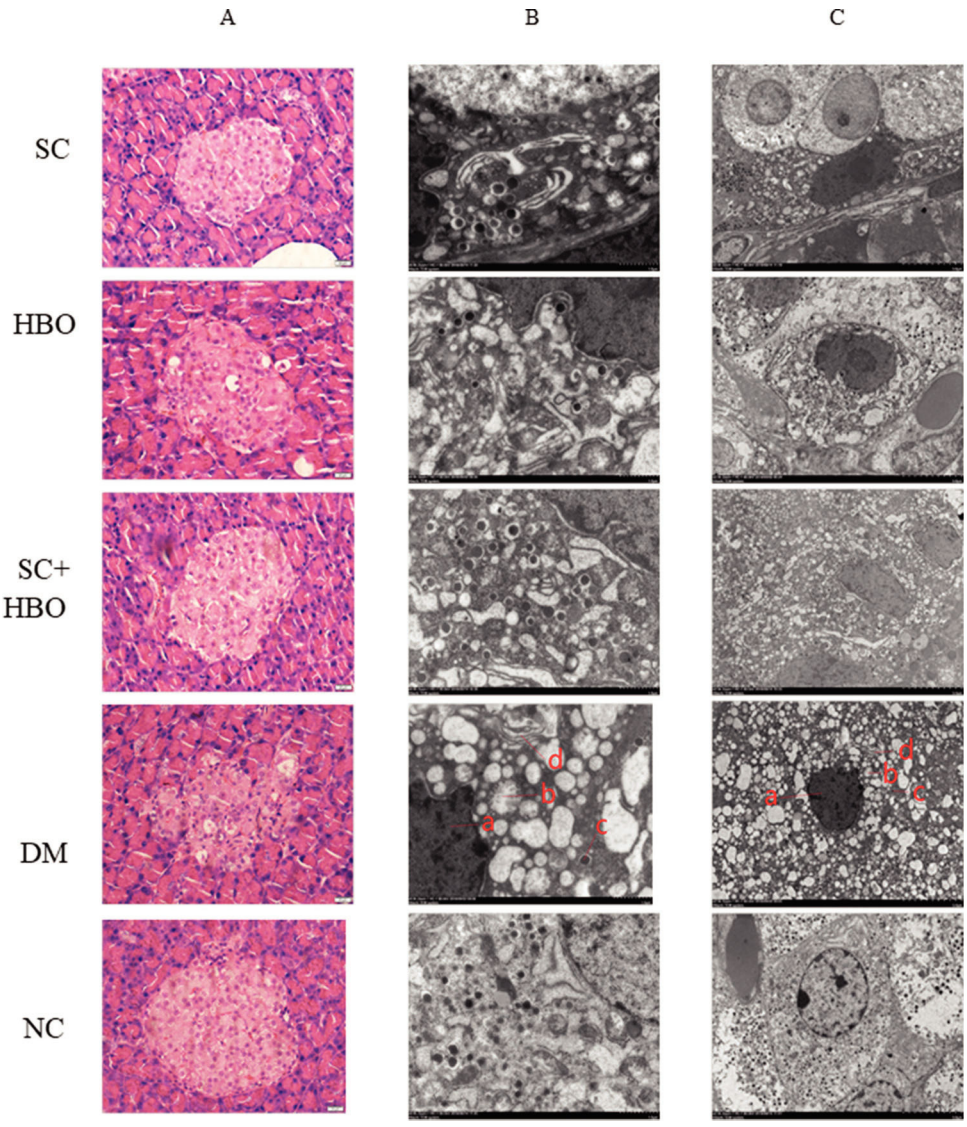

Figure 3 - Pathologic morphology of rat pancreas after 6 weeks of therapy. A. H&E staining: In the DM group, islet cells decreased and swollen cells and cytoplasmic vacuolar changes were observed; hyaline deposits were noted under the basement membrane of some islet capillaries, and inflammatory cells were scattered in the islets. The islet morphology in SC+HBO and SC groups was better than that in DM group. Scale bar: 20 μm, 400×. B. C. Electron microscopy of islet β-cells: In comparison with the β-cells in DM group, those from SC+HBO and SC groups showed decreased nuclear deformation, less swollen mitochondria, reduced lipid droplet accumulation, and significantly increased secretory granules. a. Nucleus; b. Mitochondria; c. Secretory granule; d. Ribosome. Scale bar: B.1 μm, 8000×; C. 5 μm, 2500×.

potentials, and their expression of several genes encoding extracellular and cell surface proteins may be at least twice that reported for human bone marrow MSCs (11,17). In comparison with bone marrow MSCs and permanent tooth pulp stem cells, SHED exhibit a more stable expression of genes such as basic fibroblast growth factor (*bFGF*) and bone morphogenetic protein-2 (*BMP-2*) (18,19). In addition, the dental pulp can be easily cryopreserved for a long time (20). SHED can retain their potential after cryopreservation and continue to differentiate into adult tissues after rewarming (21). Moreover, SHED can be directly extracted and cultured from the living dental pulp at any time.

Although the exact mechanism underlying the pancreatic endocrine cell development is elusive, many key regulatory factors are known to play important roles in the development of the pancreas. Pdx1 is a homeodomain transcription factor that plays a regulatory role in early development and cell maturation in the pancreas and maintains the function of mature β-cells (22,23). Pdx1 acts as a transcriptional master switch during pancreatic cell differentiation (24). It binds to the TATA box of the glucose transporter 2 (*GLUT2*) gene and participates in its transcription (25,26). Ngn3 serves as an important regulatory molecule involved in the embryonic development of β-cells of the pancreas. Ngn3 initiates the differentiation of endocrine progenitor cells (27-30) and is an important marker of islet progenitor cells (31). Pax4 is an important transcription factor for the development and regulation of the endocrine differentiation of the pancreas. It promotes the expression of transcription factors such as MafA and Nkx6.1, and induces the differentiation of

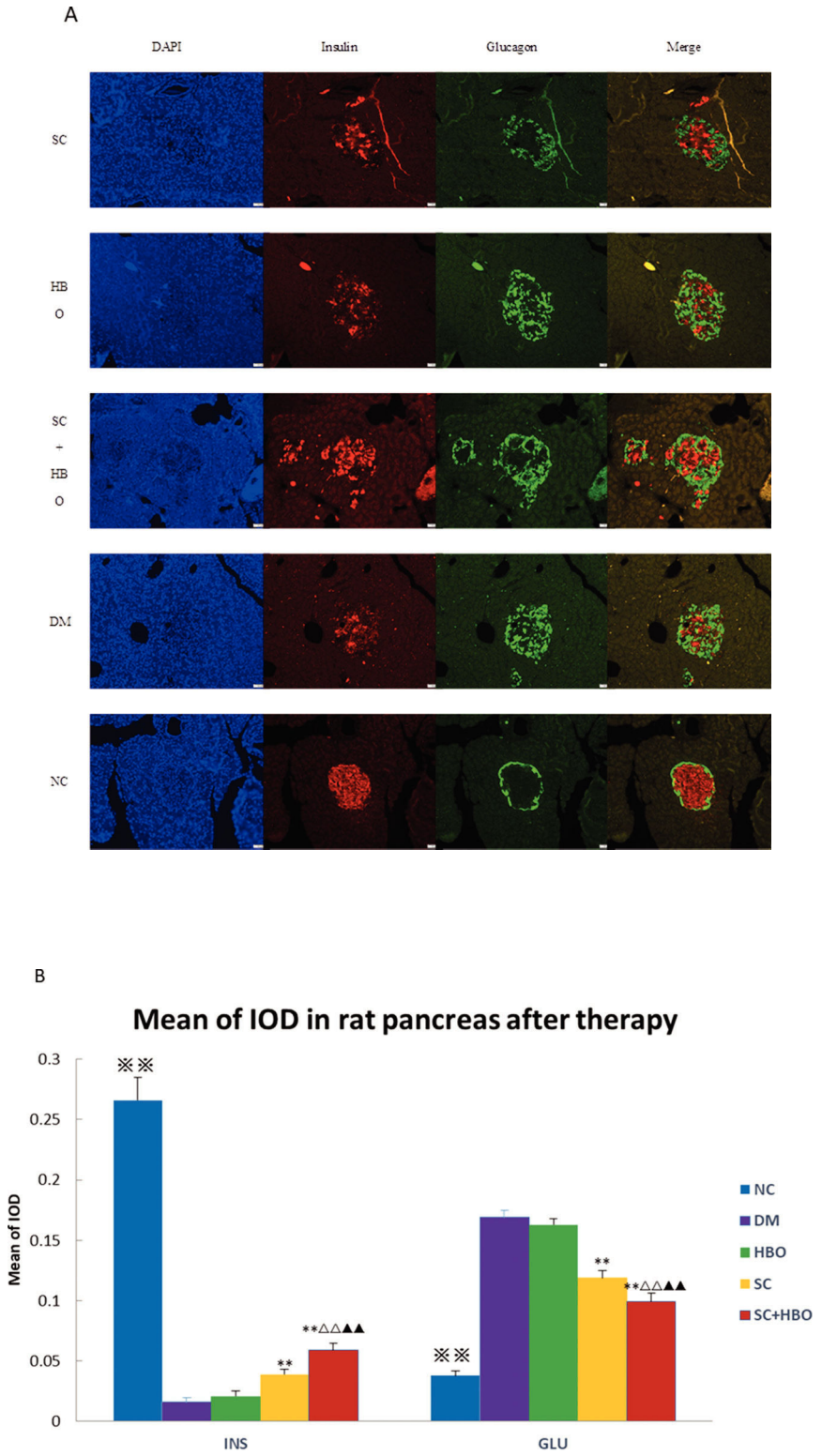

Figure 4 - Immunofluorescence analysis after 6 weeks of therapy. A. Insulin/glucagon immunofluorescence staining for pancreatic islets: In the DM group, the distribution of glucagon-positive cells (green) in the islets was disorganized, and most cells were distributed in the center and around the islets; glucagon-positive cells increased and insulin-positive cells (4) decreased as compared with those in NC group. In SC + HBO and SC groups, glucagon-positive cells in the islet center decreased and insulin-positive cells increased as compared with DM group. Scale bar: 50 μm, 200×. B. MOD of insulin or glucagon immunohistochemistry in pancreatic islets: The MOD values of insulin for SC + HBO and SC groups were higher than those for DM group. The MOD value of SC + HBO group was higher than the values for SC and HBO groups; the MOD values of glucagon for SC + HBO and SC groups were lower than the value for DM group, while the MOD value of SC + HBO group was lower than the values reported for SC and HBO groups. $^{**}p<0.01$ *vs* DM group; $^{\blacktriangle\blacktriangle}p<0.01$ *vs* SC group; $^{\triangle\triangle}p<0.01$ *vs* HBO group. $^{\divideontimes\divideontimes}p<0.01$ *vs* each of the other four groups.

pancreatic progenitor cells into endocrine cells, thereby enhancing the transcription and biosynthesis of insulin (32). Pax4 promotes the trans-differentiation of islet α-cells into β-cells (33) and reduces glucagon expression (34). It also facilitates the transformation of Pdx1-positive MSCs into islet β-cells through the regulation of the expression of Nkx6.1, MafA, and GLUT2 (35). In our study, *Pdx1*, *Ngn3*, and *Pax4* gene expression in the pancreas of SC + HBO and SC groups was significantly higher than that in the pancreas from DM group, suggesting that SHED may promote the transcription, differentiation, and development of pancreatic progenitor cells at various stages and mediate the transformation of α-cells into β-cells.

T2DM is thought to be partially associated with chronic low-grade inflammation (36). Elevated chronic inflammatory

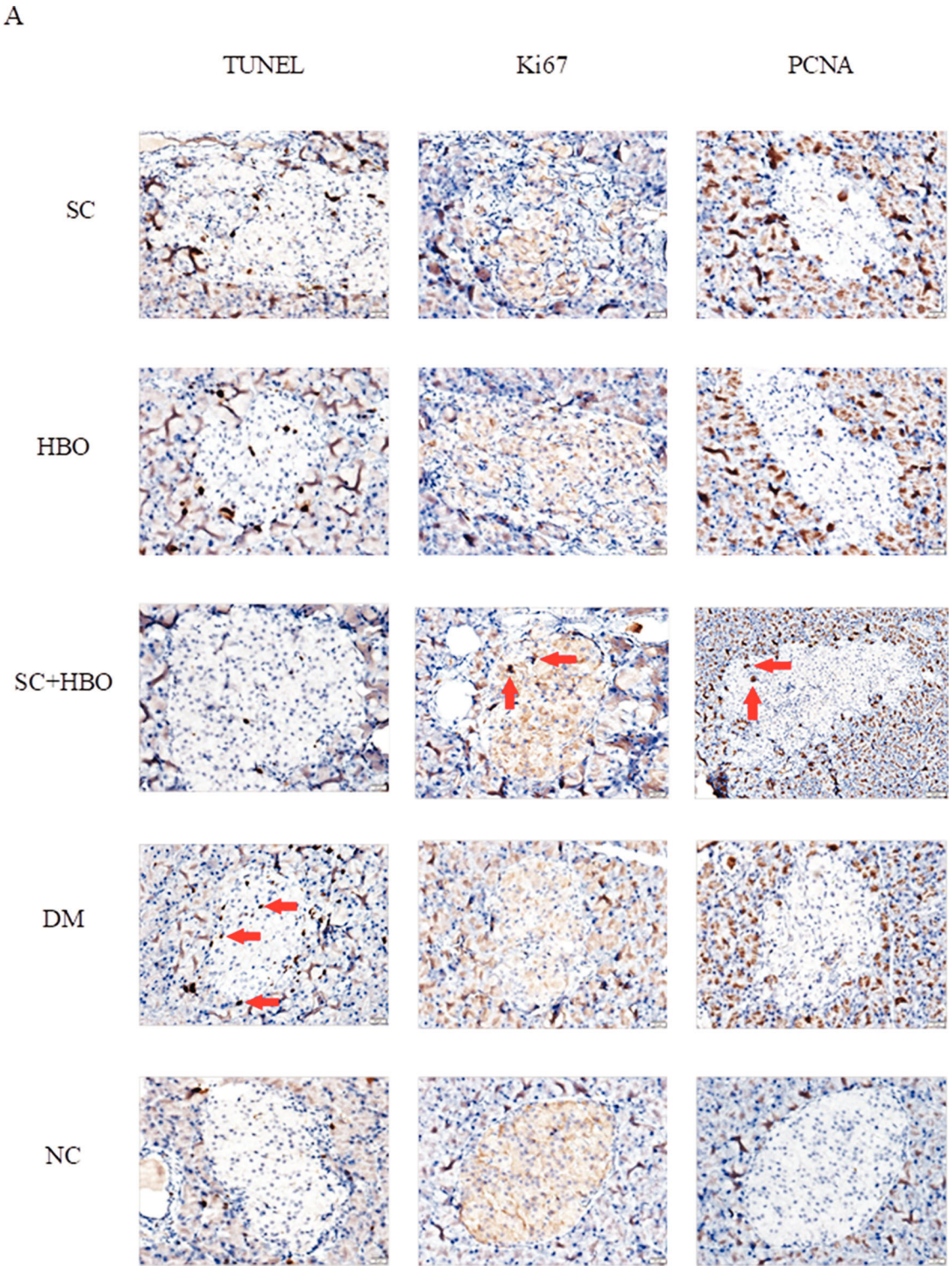

Figure 5 - Continued.

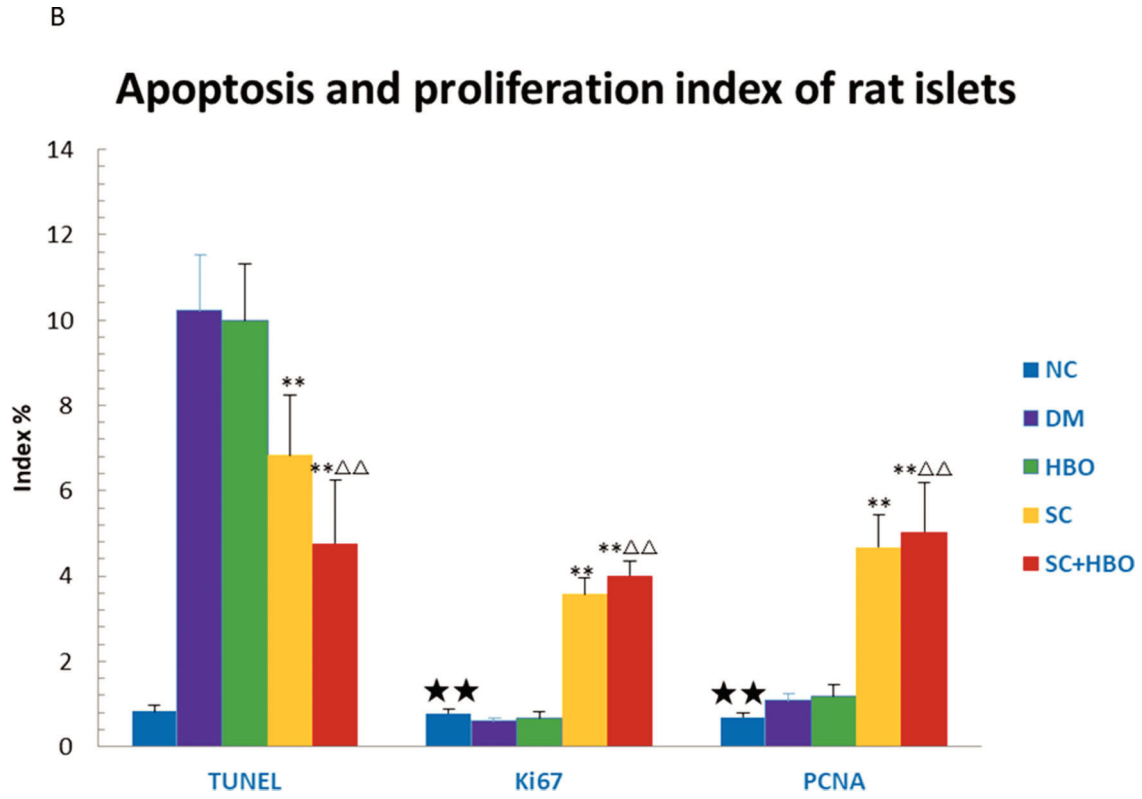

Figure 5 - Apoptosis and proliferation of pancreatic islet cells after 6 weeks of therapy. A. Staining for apoptosis and proliferation analysis in islet cells: The brown cells in the islets shown by red arrows were positively stained cells. TUNEL staining showed that the number of positively stained cells in the islets of DM group was higher than that in the islets of NC group. Positive cells in the islets of SC + HBO and SC groups were lower than those in the islets of DM group. Ki67 and PCNA staining showed that positive cells in islets were slightly higher in DM group than in NC group, and obviously increased in SC + HBO and SC groups as compared with those in DM group. Scale bar: 20 μm, 400×. B. Apoptosis index (AI) and proliferation index (PI) of islet cells: TUNEL AI was lower for SC + HBO and SC groups than that for DM group. The AI for SC + HBO group was lower than that for HBO group; the PI of Ki67 and PCNA was higher for SC + HBO and SC groups than that for DM group, while the PI of SC + HBO group was higher than that of HBO group. $^{**}p<0.01$ *vs* DM group; $^{\triangle\triangle}p<0.01$ *vs* HBO group; $^{**}p<0.01$ *vs* each of the other four groups; $^{\bigstar\bigstar}p<0.01$ *vs* either SC or SC + HBO group.

factors may decrease insulin sensitivity and induce insulin resistance, which may further impair glucose tolerance (37). Basic research and epidemiological investigation have shown the upregulated expression of TNF-α and IL-6 in subjects with T2DM (38-40). Similar changes have been observed in obese people (41). These pro-inflammatory cytokines may cause insulin resistance by blocking insulin receptor phosphorylation signaling pathway and inhibiting glucose transport (42,43). Cytokines such as TNF-α and IL-6 are key factors in the initiation of inflammation and development of insulin resistance (44,45). TNF-α infusion into healthy young male volunteers was shown to increase serum TNF-α and IL-6 levels and elevate HOMA-IR index, consequently inducing insulin resistance (46). In our study, both SC + HBO and SC groups showed significantly reduced levels of pro-inflammatory cytokines TNF-α and IL-6, consistent with the improvement in inflammatory state.

Positron emission tomography (PET) experiments using radiolabeled mouse MSCs intravenously injected in mice showed their predominant accumulation in the lungs along with a substantial level of (18)F-FDG elution from cells (47). Similar results were reported by Sood (48) in 2015. The distribution of allogeneic bone marrow-derived MSCs after intravenous injection was pathologically and bio-optically investigated by *ex vivo* imaging (using IVIS) using a fluorescent lipophilic tracer DiR; MSCs were found to be mainly distributed in the lungs and liver (49). However, a study (50) revealed the presence of BrdU-labeled MSCs in the islets after a 45-day therapy, suggestive of their pancreatic localization. In our research, SHED were not examined or found in the samples taken from rats after therapy; hence, it is unclear whether the therapeutic effect of SHED was mediated by their direct differentiation effect or secretory effect. We may speculate that SHED play therapeutic roles through secretory or immunoregulation effects by decreasing apoptosis and increasing proliferation. In our study, SHED therapy could improve the morphology of islets and β-cells, increase the number of β-cells and level of insulin secretion, and reduce α-cell number and glucagon secretion. The mechanism may involve SHED-mediated upregulation in *Pdx1*, *Pax4*, and *Ngn3* gene expression that could promote pancreatic progenitor cell differentiation into endocrine progenitor cells and islet cells, induce α-cell trans-differentiation into β-cells, and decrease the damage or apoptosis of islets by systemic or local inflammation. Further researches are warranted to explore the precise mechanism using optical *in vivo* imaging to confirm the localization and survival conditions of SHED *in vivo* or examine the cytokines secreted from SHED *in vitro* or *in vivo*. The body weights of rats from the therapy group increased with the remission of insulin resistance during the experiment; hence, remission of insulin resistance was not associated with weight loss but probably with the decrease

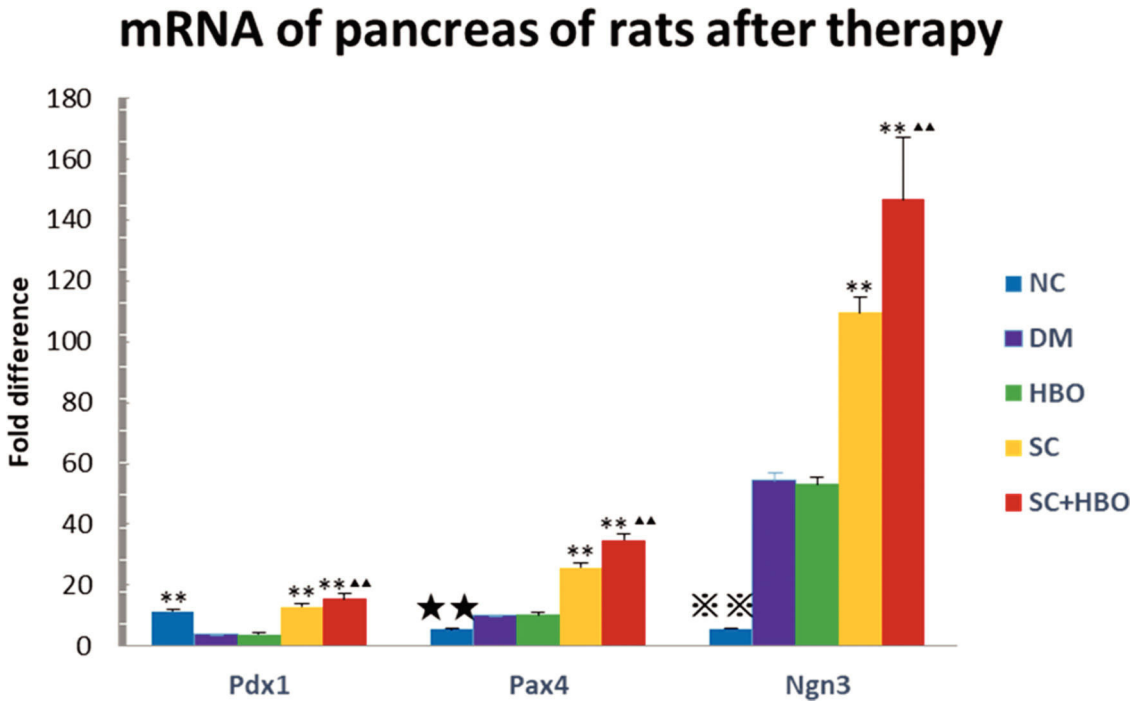

Figure 6 - Expression of *Pdx1*, *Pax4*, and *Ngn3* mRNAs in the pancreas by PCR after 6 weeks of therapy. **Gene** expression of the SC + HBO group and the SC group was higher than that of the DM group; and the expression of the SC + HBO group was higher than that of the SC group. $^{**}p<0.01$ *vs* DM group; $^{\blacktriangle\blacktriangle}p<0.01$ *vs* SC group; $^{\divideontimes\divideontimes}p<0.01$ *vs* each of the other four groups; $^{\bigstar\bigstar}p<0.01$ *vs* either SC group or SC + HBO group.

in TNF-α and IL-6 levels that improved the inflammatory status. The improvement in serum lipid and urine protein levels may also be related to the improvement in the inflammatory status of animals. A clinical trial (8) in 2008 showed that the combined therapy with intrapancreatic autologous bone marrow stem cell infusion and HBO improved the metabolic control and reduced insulin requirements in patients with T2DM. Another clinical trial (51) revealed the improvement in islet functions and metabolic control with mild adverse effects in T2DM patients subjected to autologous bone marrow mononuclear cell (BM-MNC) infusion in combination with HBO therapy; however, HBO did not synergize with BM-MNC infusion. In our experiment, HBO could reduce serum lipid, urinary protein, and serum pro-inflammatory cytokine TNF-α levels, and synergistically function with stem cells to accelerate their functions and increase the expression of pancreatic genes, thereby showing a tendency to increase therapeutic efficacy. The underlying mechanism might involve its anti-inflammatory effects, upregulation in oxidative metabolism, and improvement in oxygen supply to local hypoxic tissues.

CONCLUSION

SHED in combination with HBO therapy in T2D rats could reduce BG and HOMA-IR, increase serum insulin level, improve serum lipid level, and reduce urine protein content. The mechanism underlying the increase in insulin level may be related to the SHED-mediated upregulation in the expression of *Pdx1*, *Ngn3*, and *Pax4* in the pancreas, increase in the proliferation and secretion of pancreatic islets, enhancement in the trans-differentiation of α-cells into β-cells, and decrease in the apoptosis of islet cells. Insulin resistance may be mediated by the anti-inflammatory effects of SHED via downregulation of TNF-α and IL-6 levels. SHED combined with HBO therapy may exert synergistic effects.

ACKNOWLEDGMENTS

We thank Qingle Liu for the technical assistance with HBO, Shunmin Zhang and Canrong Ni for the technical assistance with histopathology, and Jiaqi Wang for the technical assistance with PCR. This research was supported by the National Natural Science Funds of China (81471038, 81272665).

AUTHOR CONTRIBUTIONS

Xu Y designed the study, obtained the data and wrote the manuscript. Chen J designed and performed experiments. Zhou H, Wang J, Song J, Xie J, Wang C and Guo Q performed experiments. Huang Q designed the study, edited, supported, and critically revised the manuscript and contributed to Discussion. Xu Y and Chen J contributed equally to this work. All authors have approved the final version of the manuscript to be published.

REFERENCES

1. Cho NH, Kirigia J, Claude J, Mbanya, Ogurstova K. IDF DIABETES ATLAS: Eighth edition. Abu Dhabi, UAE: International Diabetes Federation; 2017. 150 p.
2. Somani R, Jaidka S, Bajaj N, Arora S. Miracle cells for natural dentistry - A review. J Oral Biol Craniofac Res. 2017;7(1):49-53. https://doi.org/10.1016/j.jobcr.2015.11.007
3. Govindasamy V, Ronald VS, Abdullah AN, Nathan KR, Ab Aziz ZA, Abdullah M, et al. Differentiation of dental pulp stem cells into islet-like aggregates. J Dent Res. 2011;90(5):646-52. https://doi.org/10.1177/0022034510396879
4. Goldstein LJ, Gallagher KA, Bauer SM, Bauer RJ, Baireddy V, Liu ZJ, et al. Endothelial progenitor cell release into circulation is triggered by

hyperoxia-induced increases in bone marrow nitric oxide. Stem Cells. 2006;24(10):2309-18. https://doi.org/10.1634/stemcells.2006-0010
5. Thom SR, Bhopale VM, Velazquez OC, Goldstein LJ, Thom LH, Buerk DG. Stem cell mobilization by hyperbaric oxygen. Am J Physiol Heart Circ Physiol. 2006;290(4):H1378-86. https://doi.org/10.1152/ajpheart.00888.2005
6. Cechin S, Alvarez-Cubela S, Giraldo JA, Molano RD, Villate S, Ricordi C, et al. Influence of in vitro and in vivo oxygen modulation on β cell differentiation from human embryonic stem cells. Stem Cells Transl Med. 2014;3(3):277-89. https://doi.org/10.5966/sctm.2013-0160
7. Lazard D, Vardi P, Bloch K. Induction of beta-cell resistance to hypoxia and technologies for oxygen delivery to transplanted pancreatic islets. Diabetes Metab Res Rev. 2012;28(6):475-84. https://doi.org/10.1002/dmrr.2294
8. Estrada EJ, Valacchi F, Nicora E, Brieva S, Esteve C, Echevarria L, et al. Combined treatment of intrapancreatic autologous bone marrow stem cells and hyperbaric oxygen in type 2 diabetes mellitus. Cell Transplant. 2008;17(12):1295-304. https://doi.org/10.3727/096368908787648119
9. Wang L, Zhao S, Mao H, Zhou L, Wang ZJ, Wang HX. Autologous bone marrow stem cell transplantation for the treatment of type 2 diabetes mellitus. Chin Med J. 2011;124(22):3622-8.
10. Gheibi S, Kashfi K, Ghasemi A. A practical guide for induction of type-2 diabetes in rat: Incorporating a high-fat diet and streptozotocin. Biomed Pharmacother. 2017;95:605-13. https://doi.org/10.1016/j.biopha.2017.08.098
11. Sakai K, Yamamoto A, Matsubara K, Nakamura S, Naruse M, Yamagata M, et al. Human dental pulp-derived stem cells promote locomotor recovery after complete transection of the rat spinal cord by multiple neuro-regenerative mechanisms. J Clin Invest. 2012;122(1):80-90.
12. Yamaza T, Kentaro A, Chen C, Liu Y, Shi Y, Gronthos S, et al. Immunomodulatory properties of stem cells from human exfoliated deciduous teeth. Stem Cell Res Ther. 2010;1(1):5. https://doi.org/10.1186/scrt5
13. Srisawasdi S, Pavasant P. Different roles of dexamethasone on transforming growth factor-beta1-induced fibronectin and nerve growth factor expression in dental pulp cells. J Endod. 2007;33(9):1057-60. https://doi.org/10.1016/j.joen.2007.05.007
14. Iohara K, Zheng L, Ito M, Tomokiyo A, Matsushita K, Nakashima M. Side population cells isolated from porcine dental pulp tissue with self-renewal and multipotency for dentinogenesis, chondrogenesis, adipogenesis, and neurogenesis. Stem Cells. 2006;24(11):2493-503. https://doi.org/10.1634/stemcells.2006-0161
15. Jo YY, Lee HJ, Kook SY, Choung HW, Park JY, Chung JH, et al. Isolation and characterization of postnatal stem cells from human dental tissues. Tissue Eng. 2007;13(4):767-73.
16. Arora V, Arora P, Munshi AK. Banking stem cells from human exfoliated deciduous teeth (SHED): saving for the future. J Clin Pediatr Dent. 2009;33(4):289-94. https://doi.org/10.17796/jcpd.33.4.y887672r0j703654
17. Huang GT, Gronthos S, Shi S. Mesenchymal stem cells derived from dental tissues vs. those from other sources: their biology and role in regenerative medicine. J Dent Res. 2009;88(9):792-806. https://doi.org/10.1177/0022034509340867
18. Kunimatsu R, Nakajima K, Awada T, Tsuka Y, Abe T, Ando K, et al. Comparative characterization of stem cells from human exfoliated deciduous teeth, dental pulp, and bone marrow-derived mesenchymal stem cells. Biochem Biophys Res Commun. 2018;501(1):193-8. https://doi.org/10.1016/j.bbrc.2018.04.213
19. Du ZH, Li SL, Ge XY, Yu GY, Ding C. [Comparison of the secretory related molecules expression in stem cells from the pulp of human exfoliated deciduous teeth and dental pulp stem cells]. Zhonghua Kou Qiang Yi Xue Za Zhi. 2018;53(11):741-7.
20. Papaccio G, Graziano A, d'Aquino R, Graziano MF, Pirozzi G, Menditti D, et al. Long-term cryopreservation of dental pulp stem cells (SBP-DPSCs) and their differentiated osteoblasts: a cell source for tissue repair. J Cell Physiol. 2006;208(2):319-25. https://doi.org/10.1002/jcp.20667
21. Zhang W, Walboomers XF, Shi S, Fan M, Jansen JA. Multilineage differentiation potential of stem cells derived from human dental pulp after cryopreservation. Tissue Eng. 2006;12(10):2813-23. https://doi.org/10.1089/ten.2006.12.2813
22. Jonsson J, Carlsson L, Edlund T, Edlund H. Insulin-promoter-factor 1 is required for pancreas development in mice. Nature. 1994;371(6498):606-9. https://doi.org/10.1038/371606a0
23. Stoffers DA, Zinkin NT, Stanojevic V, Clarke WL, Habener JF. Pancreatic agenesis attributable to a single nucleotide deletion in the human IPF1 gene coding sequence. Nat Genet. 1997;15(1):106-10. https://doi.org/10.1038/ng0197-106
24. Talebi S, Aleyasin A, Soleimani M, Massumi M. Derivation of islet-like cells from mesenchymal stem cells using PDX1-transducing lentiviruses. Biotechnol Appl Biochem. 2012;59(3):205-12. https://doi.org/10.1002/bab.1013
25. McKenna B, Guo M, Reynolds A, Hara M, Stein R. Dynamic recruitment of functionally distinct Swi/Snf chromatin remodeling complexes modulates Pdx1 activity in islet β cells. Cell Rep. 2015;10(12):2032-42. https://doi.org/10.1016/j.celrep.2015.02.054
26. Wang X, Lei XG, Wang J. Malondialdehyde regulates glucose-stimulated insulin secretion in murine islets via TCF7L2-dependent Wnt signaling pathway. Mol Cell Endocrinol. 2014;382(1):8-16. https://doi.org/10.1016/j.mce.2013.09.003
27. Schwitzgebel VM, Scheel DW, Conners JR, Kalamaras J, Lee JE, Anderson DJ, et al. Expression of neurogenin3 reveals an islet cell precursor population in the pancreas. Development. 2000;127(16):3533-42.
28. Jensen J, Heller RS, Funder-Nielsen T, Pedersen EE, Lindsell C, Weinmaster G, et al. Independent development of pancreatic alpha- and beta-cells from neurogenin3-expressing precursors: a role for the notch pathway in repression of premature differentiation. Diabetes. 2000;49(2):163-76. https://doi.org/10.2337/diabetes.49.2.163
29. Gu G, Dubauskaite J, Melton DA. Direct evidence for the pancreatic lineage: NGN3+ cells are islet progenitors and are distinct from duct progenitors. Development. 2002;129(10):2447-57.
30. Johansson KA, Dursun U, Jordan N, Gu G, Beermann F, Gradwohl G, et al. Temporal control of neurogenin3 activity in pancreas progenitors reveals competence windows for the generation of different endocrine cell types. Dev Cell. 2007;12(3):457-65. https://doi.org/10.1016/j.devcel.2007.02.010
31. Qin Y, Xiao L, Zhan XB, Zhou HX. Pdxl and its role in activating Ngn3 and Pax6 to induce differentiation of iPSCs into islet β cells. Genet Mol Res. 2015;14(3):8892-900. https://doi.org/10.4238/2015.August.3.12
32. Napolitano T, Avolio F, Courtney M, Vieira A, Druelle N, Ben-Othman N, et al. Pax4 acts as a key player in pancreas development and plasticity. Semin Cell Dev Biol. 2015;44:107-14. https://doi.org/10.1016/j.semcdb.2015.08.013
33. Zhang Y, Fava GE, Wang H, Mauvais-Jarvis F, Fonseca VA, Wu H. PAX4 Gene Transfer Induces α-to-β Cell Phenotypic Conversion and Confers Therapeutic Benefits for Diabetes Treatment. Mol Ther. 2016;24(2):251-60. https://doi.org/10.1038/mt.2015.181
34. Gage BK, Baker RK, Kieffer TJ. Overexpression of PAX4 reduces glucagon expression in differentiating hESCs. Islets. 2014;6(2):e29236. https://doi.org/10.4161/isl.29236
35. Xu L, Xu C, Zhou S, Liu X, Wang J, Liu X, et al. PAX4 promotes PDX1-induced differentiation of mesenchymal stem cells into insulin-secreting cells. Am J Transl Res. 2017;9(3):874-86.
36. Sarangi R, Padhi S, Mohapatra S, Swain S, Padhy RK, Mandal MK, et al. Serum high sensitivity C-reactive protein, nitric oxide metabolites, plasma fibrinogen, and lipid parameters in Indian type 2 diabetic males. Diabetes Metab Syndr. 2012;6(1):9-14. https://doi.org/10.1016/j.dsx.2012.05.015
37. King GL. The role of inflammatory cytokines in diabetes and its complications. J Periodontol. 2008;79(8 Suppl):1527-34. https://doi.org/10.1902/jop.2008.080246
38. Xu H, Barnes GT, Yang Q, Tan G, Yang D, Chou CJ, et al. Chronic inflammation in fat plays a crucial role in the development of obesity-related insulin resistance. J Clin Invest. 2003;112(12):1821-30. https://doi.org/10.1172/JCI200319451
39. Guha M, Bai W, Nadler JL, Natarajan R. Molecular mechanisms of tumor necrosis factor alpha gene expression in monocytic cells via hyperglycemia-induced oxidant stress-dependent and -independent pathways. J Biol Chem. 2000;275(23):17728-39. https://doi.org/10.1074/jbc.275.23.17728
40. Morohoshi M, Fujisawa K, Uchimura I, Numano F. Glucose-dependent interleukin 6 and tumor necrosis factor production by human peripheral blood monocytes in vitro. Diabetes. 1996;45(7):954-9. https://doi.org/10.2337/diab.45.7.954
41. Popko K, Gorska E, Stelmaszczyk-Emmel A, Plywaczewski R, Stoklosa A, Gorecka D, et al. Proinflammatory cytokines Il-6 and TNF-α and the development of inflammation in obese subjects. Eur J Med Res. 2010;15 Suppl 2:120-2. https://doi.org/10.1186/2047-783X-15-S2-120
42. Chawla A, Nguyen KD, Goh YP. Macrophage-mediated inflammation in metabolic disease. Nat Rev Immunol. 2011;11(11):738-49. https://doi.org/10.1038/nri3071
43. Cani PD, Bibiloni R, Knauf C, Waget A, Neyrinck AM, Delzenne NM, et al. Changes in gut microbiota control metabolic endotoxemia-induced inflammation in high-fat diet-induced obesity and diabetes in mice. Diabetes. 2008;57(6):1470-81. https://doi.org/10.2337/db07-1403
44. Olefsky JM, Glass CK. Macrophages, inflammation, and insulin resistance. Annu Rev Physiol. 2010;72:219-46. https://doi.org/10.1146/annurev-physiol-021909-135846
45. Shree N, Bhonde RR. Conditioned Media From Adipose Tissue Derived Mesenchymal Stem Cells Reverse Insulin Resistance in Cellular Models. J Cell Biochem. 2017;118(8):2037-43. https://doi.org/10.1002/jcb.25777
46. Nielsen ST, Lehrskov-Schmidt L, Krogh-Madsen R, Solomon TP, Lehrskov-Schmidt L, Holst JJ, et al. Tumour necrosis factor-alpha infusion produced insulin resistance but no change in the incretin effect in healthy volunteers. Diabetes Metab Res Rev. 2013;29(8):655-63. https://doi.org/10.1002/dmrr.2441
47. Wolfs E, Struys T, Notelaers T, Roberts SJ, Sohni A, Bormans G, et al. 18F-FDG labeling of mesenchymal stem cells and multipotent adult

progenitor cells for PET imaging: effects on ultrastructure and differentiation capacity. J Nucl Med. 2013;54(3):447-54. https://doi.org/10.2967/jnumed.112.108316

48. Sood V, Mittal BR, Bhansali A, Singh B, Khandelwal N, Marwaha N, et al. Biodistribution of 18F-FDG-Labeled Autologous Bone Marrow-Derived Stem Cells in Patients With Type 2 Diabetes Mellitus: Exploring Targeted and Intravenous Routes of Delivery. Clin Nucl Med. 2015;40(9):697-700. https://doi.org/10.1097/RLU.0000000000000850
49. Sugiyama Y, Sato Y, Kitase Y, Suzuki T, Kondo T, Mikrogeorgiou A, et al. Intravenous Administration of Bone Marrow-Derived Mesenchymal Stem Cell, but not Adipose Tissue-Derived Stem Cell, Ameliorated the Neonatal Hypoxic-Ischemic Brain Injury by Changing Cerebral Inflammatory State in Rat. Front Neurol. 2018;9:757. https://doi.org/10.3389/fneur.2018.00757
50. Bhansali S, Kumar V, Saikia UN, Medhi B, Jha V, Bhansali A, et al. Effect of mesenchymal stem cells transplantation on glycaemic profile & their localization in streptozotocin induced diabetic Wistar rats. Indian J Med Res. 2015;142(1):63-71. https://doi.org/10.4103/0971-5916.162116
51. Wu Z, Cai J, Chen J, Huang L, Wu W, Luo F, et al. Autologous bone marrow mononuclear cell infusion and hyperbaric oxygen therapy in type 2 diabetes mellitus: an open-label, randomized controlled clinical trial. Cytotherapy. 2014;16(2):258-65. https://doi.org/10.1016/j.jcyt.2013.10.004